Molecular Therapy
Nucleic Acids
Original Article

An aptamer interacting with heat shock protein 70 shows therapeutic effects and prognostic ability in serous ovarian cancer

Chang-Ni Lin,[1,8] Yi-Cheng Tsai,[2,8] Ching-Cheng Hsu,[3] Yu-Ling Liang,[1] Yi-Ying Wu,[4] Chieh-Yi Kang,[5] Chun-Hong Lin,[5] Pang-Hung Hsu,[6,7] Gwo-Bin Lee,[2] and Keng-Fu Hsu[1]

[1]Department of Obstetrics and Gynecology, National Cheng Kung University Hospital, College of Medicine, National Cheng Kung University, Tainan, Taiwan; [2]Department of Power Mechanical Engineering, National Tsing Hua University, Hsinchu, Taiwan; [3]Department of Radiation Oncology, University of Texas Southwestern Medical Center at Dallas, Dallas, TX, USA; [4]Graduate Institute of Clinical Medicine, College of Medicine, National Cheng Kung University, Tainan, Taiwan; [5]Department of Obstetrics and Gynecology, Chi-Mei Medical Center, Tainan, Taiwan; [6]Department of Bioscience and Biotechnology, National Taiwan Ocean University, Keelung, Taiwan; [7]Institute of Biochemistry and Molecular Biology, National Yang Ming University, Taipei, Taiwan

Ovarian cancer (OvCa) is the most lethal gynecologic malignancy owing to its high chemoresistance and late diagnosis, which lead to a poor prognosis. Hence, developing new therapeutic modalities is important for OvCa patient treatment. Our previous results indicated that a novel aptamer, Tx-01, can specifically recognize serous carcinoma cells and tissues. Here, we aim to clarify the clinical role and possible molecular mechanisms of Tx-01 in OvCa. Immunostaining and statistical analysis were performed to detect the interaction of Tx-01 and heat shock protein 70/Notch1 intracellular domain (HSP70/NICD) in OvCa. The *in vitro* and *in vivo* experiments were carried out to demonstrate the potential mechanisms of Tx-01. Results show that Tx-01 reduced serous OvCa OVCAR3 cell migration and invasion and inhibited HSP70 nuclear translocation by interrupting the intracellular HSP70/NICD interaction. Furthermore, Tx-01 suppressed serous-type OVCAR3 cell tumor growth *in vivo*. Tx-01 acts as a prognostic factor through its interaction with membrane-bound HSP70 (mHSP70 that locates on the cell surface without direct interaction to NICD) on ascitic circulating tumor cells (CTCs) and is reported to be involved in natural killer (NK) cell recognition and activation. Our data demonstrated that Tx-01 interacted with HSP70 and showed therapeutic and prognostic effects in serous OvCa. Tx-01 might be a potential inhibitor for use in serous OvCa treatment.

INTRODUCTION

Ovarian cancer (OvCa) is the most lethal type of gynecological cancer because of difficulties in early detection and chemoresistance.[1] Even though thorough surgical removal of the tumor can be performed, the risk for recurrence of OvCa remains as high as 60%.[2] Among the different histologic types of OvCas, high-grade serous cancer is the most common and lethal form of OvCa.[3] Recently, targeting homologous recombination deficiency (HRD), a molecular hallmark in approximately 50% of high-grade serous OvCa, poly (ADP-ribose) polymerase inhibitors can improve outcomes for a substantial number of women with OvCa.[4] However, due to the high cost of new cancer therapies and a non-HRD subgroup of serous OvCa, developing new treatment modalities and predictive markers is mandatory.

Aptamers, short nucleic acids that can be selected through single-stranded DNA (ssDNA) or RNA library binding onto a specific target molecule *in vitro*, are used to bind targets with high affinity and specificity.[5] One of the greatest advantages of aptamers for both diagnostic and therapeutic applications is their relatively small size. The average aptamer is approximately 10- to 15-fold smaller than a monoclonal antibody. The selection process is termed the systematic evolution of ligands by exponential enrichment (SELEX). Currently, aptamer applications in clinical diagnosis provide several advantages, such as high specificity and selectivity, ease of synthesis, and relatively low production costs, compared with antibodies produced from animal serum. Therefore, they have been suggested for use in cancer diagnosis. For instance, Meirinho et al.[6] selected a DNA aptamer as a potential aptasensor against osteopontin in the plasma of patients with breast cancer, and the sensitivity was reported to be better than that of the standard ELISA method. Previously, we demonstrated that Tx-01 is a highly specific aptamer that recognizes serous OvCa cells on glass slides in a microfluidic system with automated SELEX.[7,8] However, the biological effects of Tx-01 in OvCa were unclear.

Heat shock protein 70 (HSP70) is usually highly expressed in cancer cells and is commonly associated with disease progression.[9,10]

Received 30 August 2020; accepted 31 December 2020;
https://doi.org/10.1016/j.omtn.2020.12.025.

[8]These authors contributed equally

Correspondence: Keng-Fu Hsu, MD, PhD, Department of Obstetrics and Gynecology, National Cheng Kung University Hospital, College of Medicine, National Cheng Kung University, Tainan, Taiwan.
E-mail: d5580@mail.ncku.edu.tw
Correspondence: Gwo-Bin Lee, PhD, Department of Power Mechanical Engineering, National Tsing Hua University, Hsinchu, Taiwan.
E-mail: gwobin@pme.nthu.edu.tw

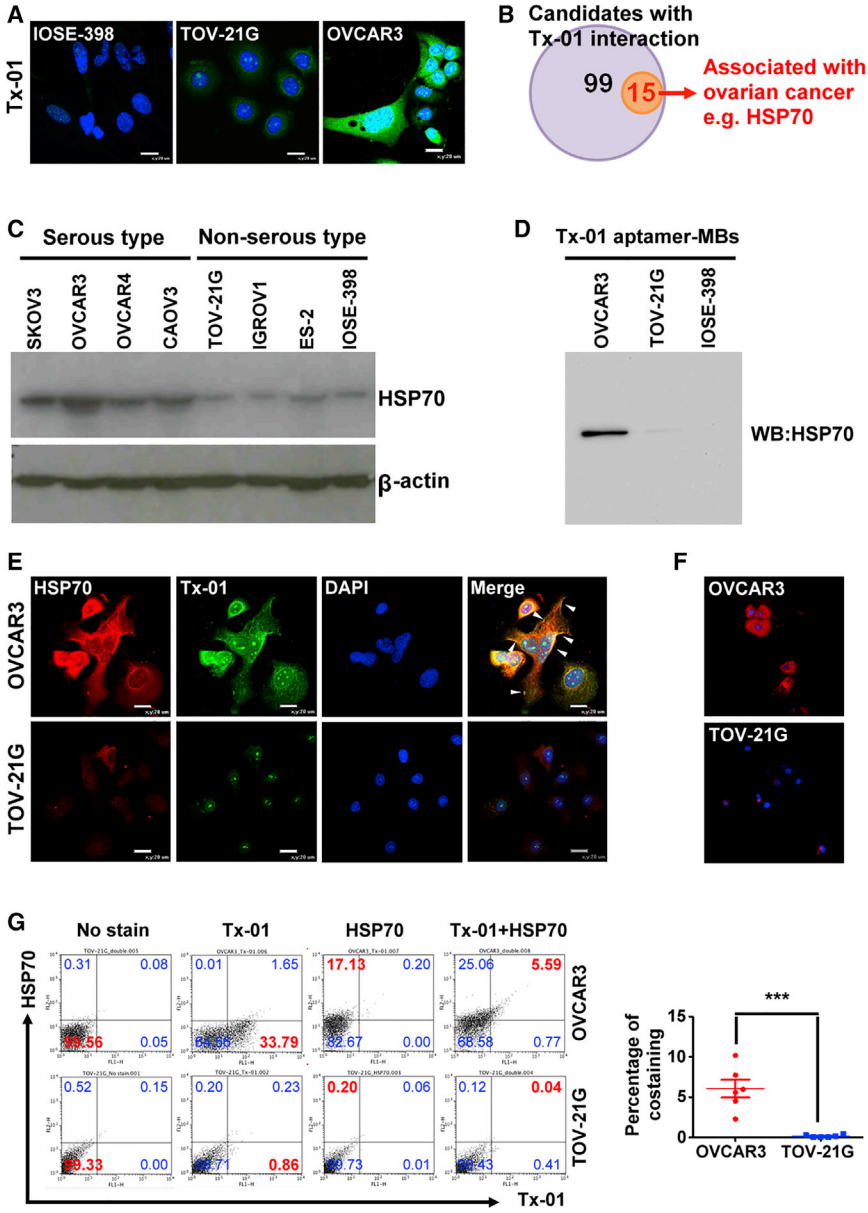

Figure 1. Heat shock protein 70 (HSP70) interacted with the Tx-01 aptamer in serous OvCa

(A) Immunofluorescence-stained Tx-01 was abundant in the OVCAR3 cells (serous OvCa cell line) compared with that in the IOSE-398 cells (normal ovarian epithelium cells) or TOV-21G cells (clear cell OvCa cell line) staining. (B) 99 candidates interacting with the Tx-01 aptamer were identified by liquid chromatography/tandem mass spectrometry (LC-MS/MS) and included 15 candidates related to ovarian cancer, such as HSP70. (C) HSP70 expression was higher in the serous OvCa cell lines than in the non-serous OvCa cell lines. (D) Tx-01 aptamer-conjugated magnetic beads (Tx-01 aptamer-MBs) and anti-human HSP70 antibody were used to demonstrate the interaction of Tx-01 and HSP70 in OVCAR3 and TOV-21G cells through pull-down assay. The interaction of Tx-01 and HSP70 in the OVCAR3 cells was stronger than that in TOV-21G cells. Random ssDNA-conjugated MBs (random ssDNA-MBs) as the negative control. (E) Confocal microscopy images showed that the colocalization of HSP70 (red) and Tx-01 (green) in the OVCAR3 cells was more obvious than that in the TOV-21G cells. Scale bar, 20 μm. Arrows indicate the colocalization of Tx-01 and HSP70 in the cell membrane. (F) Duolink proximity ligation assay (PLA) showed that the interaction of Tx-01 and HSP70 in the OVCAR3 cells was stronger than that in the TOV-21G cells. (G) The Tx-01 aptamer and HSP70 interaction in the OVCAR3 cells was significantly higher than that in the TOV-21G cells, according to the flow cytometry analyses. ***$p < 0.01$.

Approximately 15% to 20% of the total cellular HSP70 is found on the plasma membrane of some tumor cells, called membrane-bound HSP70 (mHSP70), which may be due to its highly specific affinity for cholesterol and phosphatidylserine.[11–14] mHSP70 has been reported to act as a novel circulating tumor cell marker because it is the only member of the HSP family found on the cell surface, especially on cancer cells.[15,16] Furthermore, mHSP70 has been found to have a tumor-specific structure recognized by natural killer (NK) cells, which stimulates the cytolytic and proliferative activity of the NK cells, and has been found to kill cancer cells expressing membrane HSP70.[17,18] Additionally, the frequency of NK cells within the lymphocyte fraction in ascites at diagnosis is related to the survival of OvCa patients.[19]

The Notch pathway is involved in cell proliferation, differentiation, and survival and is one of the most commonly activated signaling pathways in many cancers, including OvCa.[20–22] It was reported that HSP70 can interact with the Notch1 intracellular domain (NICD) to activate Notch signaling.[23] HSP70 may play a dual role in the cell surface recognition by NK cells and intracellular signal regulation of OvCa. Considering the liquid chromatography/tandem mass spectrometry (LC-MS/MS) analysis, we hypothesize that Tx-01 may interact with HSP70, and we thus sought to clarify the clinical implications of Tx-01 and its possible molecular mechanism in OvCa.

RESULTS

Tx-01 interacted with HSP70 in serous OvCa cells

To explore the possible mechanism by which Tx-01 recognizes serous OvCa, we first used immunofluorescence staining to study the correlation of Tx-01 and cell types. We noticed that the binding of Tx-01 on OVCAR3 serous-type OvCa cells was more abundant than that on normal IOSE-398 ovarian cells or TOV-21G non-serous-type OvCa cells (Figure 1A). Through LC-MS/MS analysis, 99 candidates were identified, of which 15 candidates were associated with OvCa (Figure 1B; Table S1). HSP70 was found to be the most likely candidate

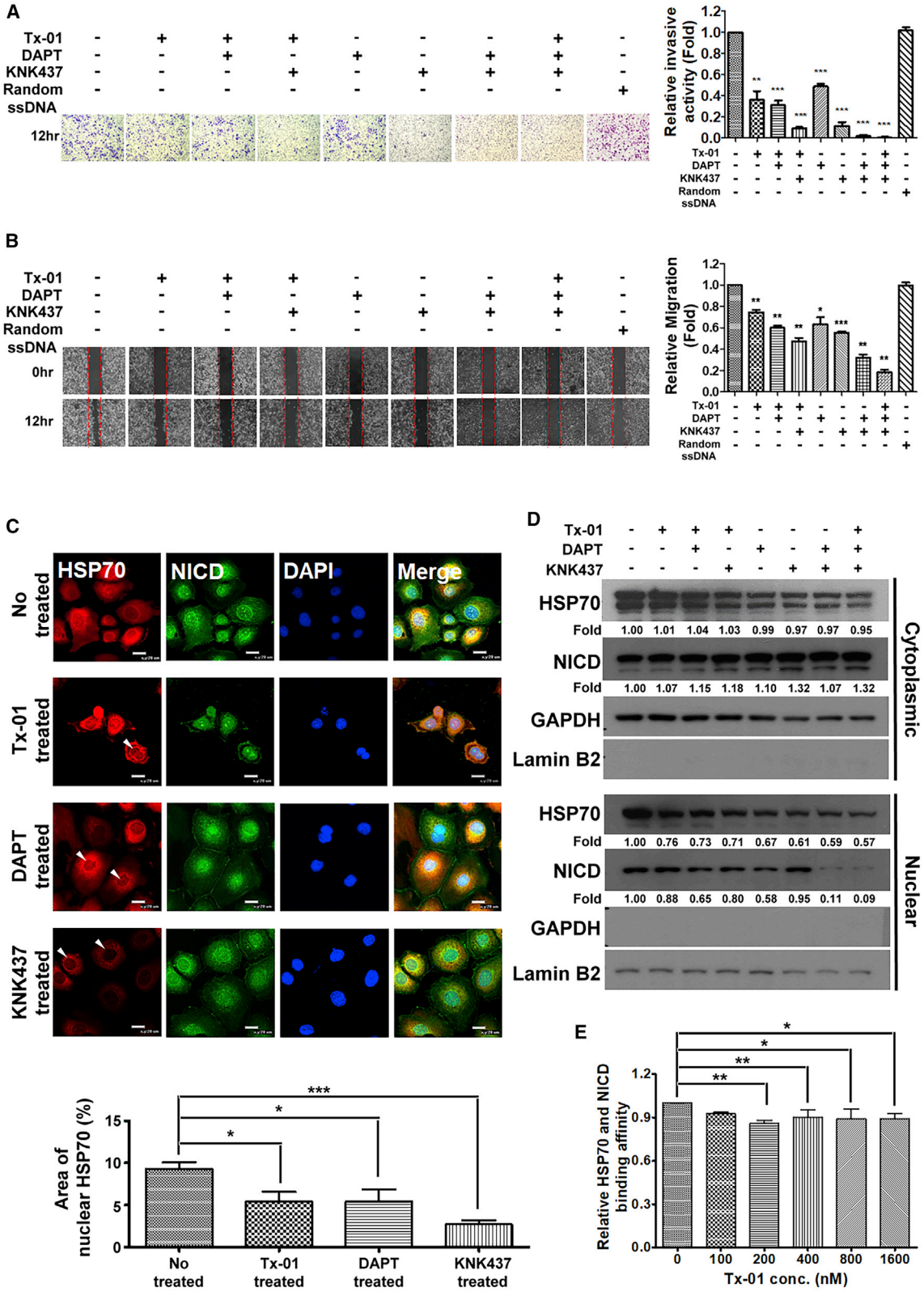

(legend on next page)

by which Tx-01 binds to OVCAR3 cells, especially because it was reported to be expressed not only in the cytoplasm and nucleus but also on the cell membrane.[13] Therefore, we selected HSP70 for use in subsequent experiments performed to validate our hypothesis. We excluded the candidate with the highest score, histone 2B type 1J (H2B1J), because of its expressed location. No reports have indicated that H2B1J is expressed on the cell membrane and that histone H2B ubiquitination is essential for tumor suppression in OvCa.[24] The western blotting data also showed that the serous-type OC cell line, i.e., OVCAR3, SKOV3, and CAOV3, exhibited more HSP70 expression compared with other non-serous type cell lines (Figure 1C).

To demonstrate the interaction of HSP70 and Tx-01, we next performed an immunoprecipitation assay using magnetic beads (MBs) coated with Tx-01 aptamers (i.e., Tx-01 aptamer-MBs) to capture target cancer cells, as well as normal ovarian epithelial cells, IOSE-398. The interaction of Tx-01 and HSP70 on the serous-type OVCAR3 cells was found to be obvious more than it was on the non-serous-type TOV-21G cells and normal ovarian IOSE-398 cells (Figure 1D). The confocal images showed that HSP70 was diffusely distributed in the cytoplasm; another critical feature was the aggregation of HSP70 on the cell surface, with a few HSP70 molecules located in the nucleus (Figure 1E, red fluorescence). On the other hand, Tx-01 (Figure 1E, green fluorescence) was abundantly distributed in the cytoplasm and nucleus. Notably, the sporadic signals of Tx-01 and HSP70 were colocalized on the cell surface (arrowhead). Moreover, a proximity ligation assay (PLA) indicated that the interaction of Tx-01 and HSP70 was much stronger in the OVCAR3 cells than it was in the TOV-21G cells (Figure 1F). In addition, Tx-01 aptamer could directly interact with recombinant human HSP70 protein in ELISA assay (Figure S1A). Figures S1By utilizing flow cytometry, we also demonstrated that if without the permeation step during the process of immunocytochemistry staining preparation, Tx-01 recognized HSP70 on the OVCAR3 cell surface (Figure 1G) less than10%. However, when the permeation step existenced in the process of immunocytochemistry staining preparation, the interaction of Tx-01 and HSP70 were obviously increased (Figures S1B and S1C). These results suggest that Tx-01 interactions with HSP70 may play an important role in serous OvCa.

Tx-01 inhibited OVCAR3 cell proliferation, migration, and invasion by interrupting the interaction of HSP70 and the NICD

HSP70 has been reported to play a critical role in cancer development and has a positive correlation with increased cell proliferation and malignancy.[9] In addition, it has been demonstrated that HSP70 interacts with the NICD and then is translocated into the nucleus to regulate Notch signals.[23] Here, we aimed to clarify whether Tx-01 was involved in the HSP70/NICD signaling pathway to regulate biological functions in OVCAR3 cells. Thus, we used γ-secretase inhibitor (DAPT) or HSP70 inhibitor (KNK437) to block HSP70 and Notch1 interaction. The optimal Tx-01 working concentration was selected by (3-(4,5-dimethylthiazol-2-yl)-2,5-diphenyltetrazolium bromide) (MTT) assay (Figure S2A). OVCAR3 cell invasion was found to be significantly reduced after treatment with 200 nM Tx-01 compared with that of the untreated cells, while there was no inhibition of invasion in the random ssDNA treatment (in 200 nM; Figure 2A). Similarly, the wound-healing assay showed that Tx-01 contributed to reduce cell migration ability, a result similar to that after inhibitor treatment (Figure 2B). In addition, we used MTT assay to confirm the Tx-01 could inhibit cell proliferation at 12 and 24 h treatment (Figure S2B). All the inhibitors, DAPT, KNK437, or Tx-01 could inhibit cell proliferation, migration, and invasion, especially in combined treatment (Figures 2A and 2B; Figure S2B). Confocal microscopic images also showed that the HSP70 expression signal intensity was significantly reduced in the OVCAR3 cell nuclei (arrowhead) after Tx-01, DAPT, or KNK437 treatment (Figure 2C). Furthermore, the nuclear expression of HSP70 and NICD was reduced in the OVCAR3 cells after inhibitor treatment (Figure 2D, lanes 3–8). Significantly, the same phenomena were also observed after Tx-01 treatment (Figure 2D, lane 2). We next used recombinant human HSP70 to serve as an antigen to detect the binding affinity of HSP70 with NICD with/without Tx-01 exposure. According to the ELISA result, the HSP70 and NICD binding affinity was significantly decreased after exposure to 200 nM Tx-01 (Figure 2E), implying that Tx-01 may act as an inhibitor that interrupts the interaction of HSP70/NICD and then blocks HSP70 translocation into the nucleus.

Tx-01 inhibited serous OvCa tumor growth with reduced HSP70 nuclear translocation and increased apoptosis in a xenograft model, and low nuclear HSP70 expression is associated with good prognosis in serous OvCa patients

Xenograft model mice were randomly allocated into 3 groups: group A, group B, and group C, with group A serving as the control group. Next, we pretreated OvCa cells with Tx-01 (200 nM) for 12 h and then subcutaneously injected the cells (1×10^6 cells) into nude mice (groups B and C). After inoculation, the group C mice were administered Tx-01 (200 nM) twice weekly. On average, the TOV-21G xenograft tumor size and growth rate were larger and faster, respectively, than they were in the OVCAR3 xenograft tumors (Figures 3A

Figure 2. Tx-01 is an inhibitor that interrupts the interaction of intracellular HSP70 and the Notch1 intracellular domain (NICD) to suppress OVCAR3 cell migration and invasion

(A and B) After Tx-01 (200 nM), DAPT (γ-secretase inhibitor, 5 μg/mL), and KNK437 (HSP70 inhibitor, 100 μM) treatment, cell migration and invasion were significantly reduced in the OVCAR3 cells compared with the untreated cells. Random ssDNA treatment was used as the negative control. Quantification of cell migration (A, right side) and invasion (B, right side) was performed using ImageJ software. *$p < 0.05$; **$p < 0.01$; ***$p < 0.001$. (C) Immunofluorescence stain was used to observe the nuclear translocation of HSP70-NICD. After DAPT or KNK437 treatment, HSP70 translocation into the nuclei was obviously reduced. The triangle indicates nuclear HSP70, and the arrow indicates membrane HSP70 in the untreated group (scale bar, 20 μm). Quantification of nuclear HSP70 expression was performed using ImageJ software. *$p < 0.05$; **$p < 0.01$; ***$p < 0.001$. (D) Western blot assay was used to confirm that nuclear HSP70 and NICD were obviously reduced after Tx-01, DAPT, or KNK437 treatment. (E) The binding affinity of HSP70 and NICD was significantly reduced after 200 nM, 400 nM, 800 nM, and 1,600 nM Tx-01 treatment. *$p < 0.05$; **$p < 0.01$.

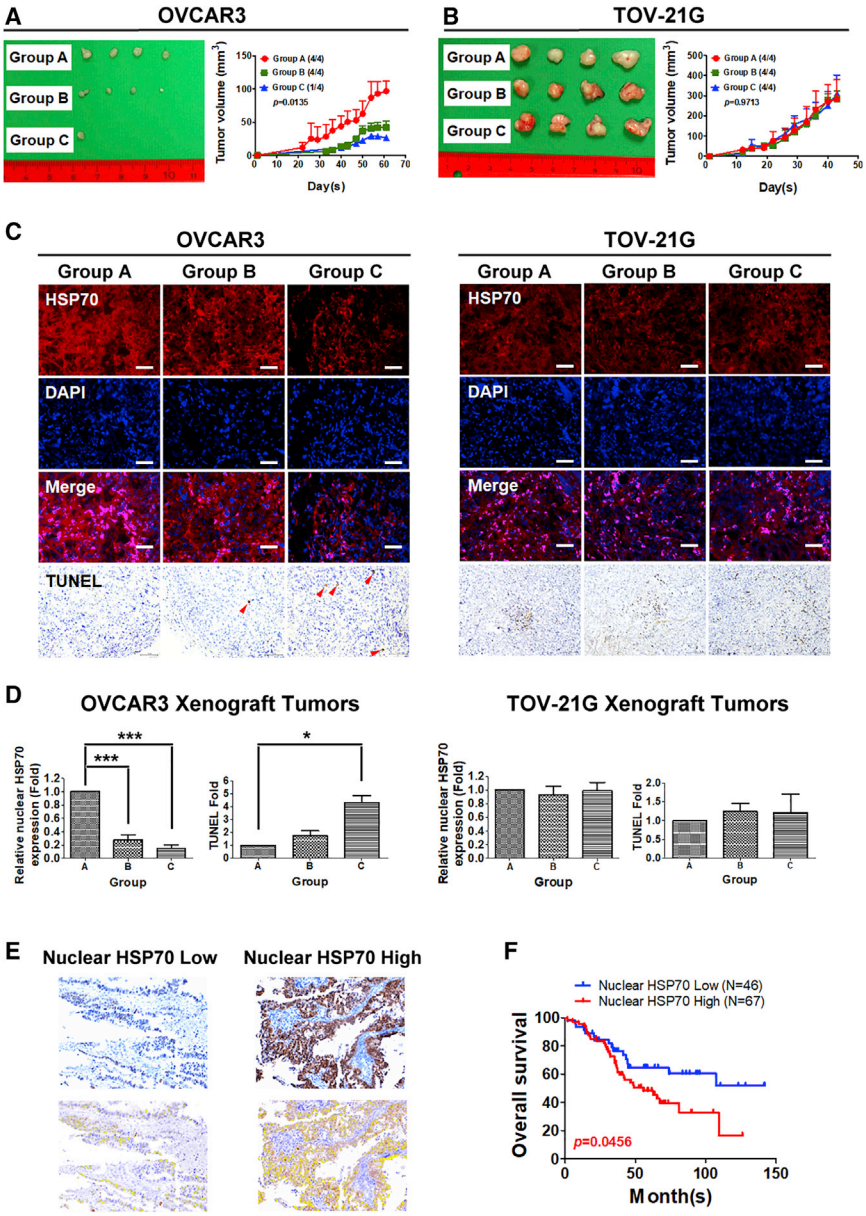

Figure 3. Tx-01 inhibited OvCa tumor growth in a xenograft mouse model

Serous OvCa patients with high nuclear expression of HSP70 carried poor prognosis. (A and B) Group A, untreated; group B, pretreatment with Tx-01 200 nM for 12 h; group C, Tx-01 200 nM treated twice per week. The OVCAR3 xenograft tumor sizes in groups B and C were significantly smaller and grew more slowly than those of group A (one-way ANOVA; p = 0.0135). The TOV-21G xenograft tumor size and growth rate were not significantly different (one-way ANOVA; p = 0.9713). (C and D) Fluorescence microscopy images showing that nuclear HSP70 was significantly reduced in OVCAR3 xenograft tumors of groups B and C compared with group A OVCAR3 xenograft tumors. The number of apoptotic cells was significantly increased in group C. No significant difference was noted in the TOV-21G xenograft tumors. Scale bar, 100 μm. Quantification of nuclear HSP70 expression was performed using Nuance analysis software based on attachments observed via microscopy. *p < 0.05; **p < 0.01; ***p < 0.001. (E) Nuclear HSP70 was observed in serous carcinoma after IHC staining. Images indicate low and high nuclear HSP70. Scale bar, 200 μm. (F) Serous OvCa patients with high nuclear HSP70 expression had poor overall survival (p = 0.0456).

and 3B). OVCAR3 xenograft tumor sizes in groups B and C were significantly smaller, with the tumors growing more slowly compared with the size and growth of the group A tumors (no treatment; Figure 3A). However, the TOV-21G xenograft tumors size and growth rate were not different between these three groups (Figure 3B). Moreover, there is no significant reduction of tumor size in OVCAR3 xenograft under the treatment of random ssDNA (Figure S3A). After immunofluorescence staining, we observed in the fluorescence microscopy images that the expression level of nuclear HSP70 was different in the 3 groups. As expected, nuclear HSP70 expression was obviously reduced in group C OVCAR3 xenograft tumors, and this reduction was correlated with increased cell apoptosis (Figure 3C, left). The quantitative results are shown in Figure 3D and suggest that Tx-01 contributed to the inhibited intracellular HSP70 translocation into the nucleus, which suppressed cell proliferation and induced cell apoptosis. We next tested whether Tx-01, DAPT, and KNK437 could induce OvCa cell apoptosis *in vitro*. The results showed that all Tx-01, DAPT, and KNK437, as well as combination treatments, could induce OVCAR3 cell apoptosis by fluorescence-activated cell sorting (FACS) assay (Figures S3B and S3C).

A cohort of 113 patients with serous OvCa, including 54 patients from National Cheng Kung University Hospital (NCKUH), Taiwan, and 59 patients from Chi Mei Hospital (CMH), Taiwan, was recruited to obtain samples for HSP70 immunohistochemistry (IHC) staining, for studying clinical associations. The clinical characteristics of these samples are described in Table S3. Quantitation of nuclear HSP70 levels was determined by Nuance imaging software (version 3.0.2, PerkinElmer) based on three views of 200× field. A time-dependent receiver operating characteristic curve (ROC) was used to determine the best cutoff point and distinguish nuclear HSP70 low expression (≤2.3) from high expression (>2.3; microscopy images shown in Figure 3E). The survival analysis results showed that high nuclear HSP70 expression was significantly associated with a poor outcome (p = 0.0456; Figure 3F). In summary, nuclear HSP70 translocation is essential for serous OvCa progression, while Tx-01 contributes to the inhibition of nuclear HSP70 translocation by interfering with the

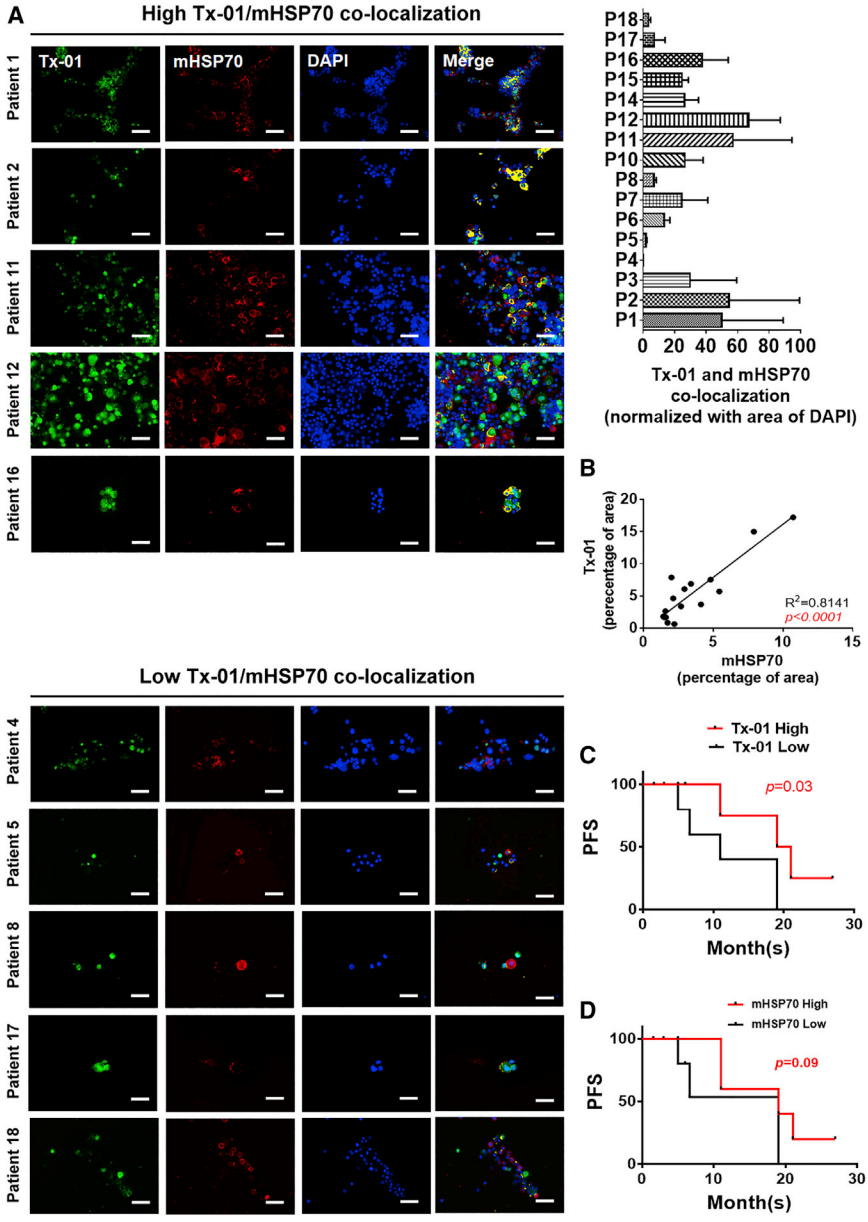

Figure 4. Tx-01 recognized membrane-bound HSP70 (mHSP70) on the circulating tumor cells (CTCs) in ascites and led to favorable prognosis

(A) Representative fluorescence microscopy images showing Tx-01 and mHSP70 colocalization in the EpCAM(+) CTCs from serous OvCa patient ascites. Scale bar, 100 μm. Right upper graph shows the summary of Tx-01 and HSP70 colocalization percentage in all 16 ascites samples. (B) Tx-01 expression in the ascitic CTCs was significantly correlated with mHSP70 ($p < 0.0001$; $R^2 = 0.8141$). (C) High Tx-01 binding in the ascitic CTCs was significantly associated with higher PFS ($p = 0.03$). (D) High mHSP70 expression in the ascitic CTCs was associated with borderline favorable PFS compared with low mHSP70 expression ($p = 0.09$). PFS, progression-free survival.

interaction of HSP70 and NICD. Therefore, Tx-01 has therapeutic potential in serous OvCa by blocking HSP70 nuclear translocation.

Tx-01 recognized mHSP70 in serous OvCa ascitic circulating tumor cells (CTCs) and led to favorable prognosis

Considering these results, we next used magnetic beads with surface-coated anti-human EpCAM antibody to isolate CTCs in ascites from 16 OvCa patients for use in immunofluorescence staining to verify the cell surface interactions. The clinical information of 16 patients is described in Table S2 and includes 1 patient (Patient 8) whose sample was obtained at the 2nd surgery during tumor recurrence, which was excluded from the survival analysis. The flow chart showing the experimental design for the ascitic CTC and EpCAM (–) cell analyses is presented in Figure S4-1. The results of EpCAM-MB isolation enrichment from the 16 OvCa patient samples are shown in Figure S4-2. There were 4 patients CTCs with no EpCAM enrichment. We used a specific anti-human mHSP70 antibody (sc-66048; Santa Cruz Biotechnology) to verify the cell-surface binding of Tx-01 and mHSP70. The percentage of areas stained for Tx-01 and mHSP70, including areas of co-localization, was calculated based on three different fields magnified at 200× with Nuance imaging software (version 3.0.2, PerkinElmer). We observed that Tx-01 (green fluorescence) and mHSP70 (red fluorescence) were co-localized on the cell surface of ascitic CTCs (Figure 4A) with some variation, which could be categorized as high and low colocalization areas based on the median percentage area (=0.45; yellow). Moreover, the individual binding area of Tx-01 in the ascitic CTCs was significantly correlated with the mHSP70 area ($p < 0.0001$; $R^2 = 0.8141$; Figure 4B). To determine whether Tx-01 is a prognostic factor, we divided the CTCs into high-Tx-01-binding or low-Tx-01-binding groups according to the median percentage area (=4.19). Patients with high Tx-01 binding in ascitic CTCs had significantly more favorable progression-free survival (PFS) than those with low Tx-01 binding ($p = 0.03$; Figure 4C). However, when using the median percentage area (=2.45) of the mHSP70 as the cutoff value, patients with high mHSP70 expression in ascitic CTCs were associated with borderline favorable PFS compared with those with low mHSP70 expression ($p = 0.09$; Figure 4D).

Tx-01 binding in ascitic CTCs was positively correlated with CD56(+)CD107a(+) NK cells, and high CD56(+)CD107a(+) NK cells led to a favorable prognosis for serous OvCa patients

Because mHSP70 was reported to be recognized by NK cells and to lead to mHSP70(+) tumor cells being killed by NK cells,[17,18] we next

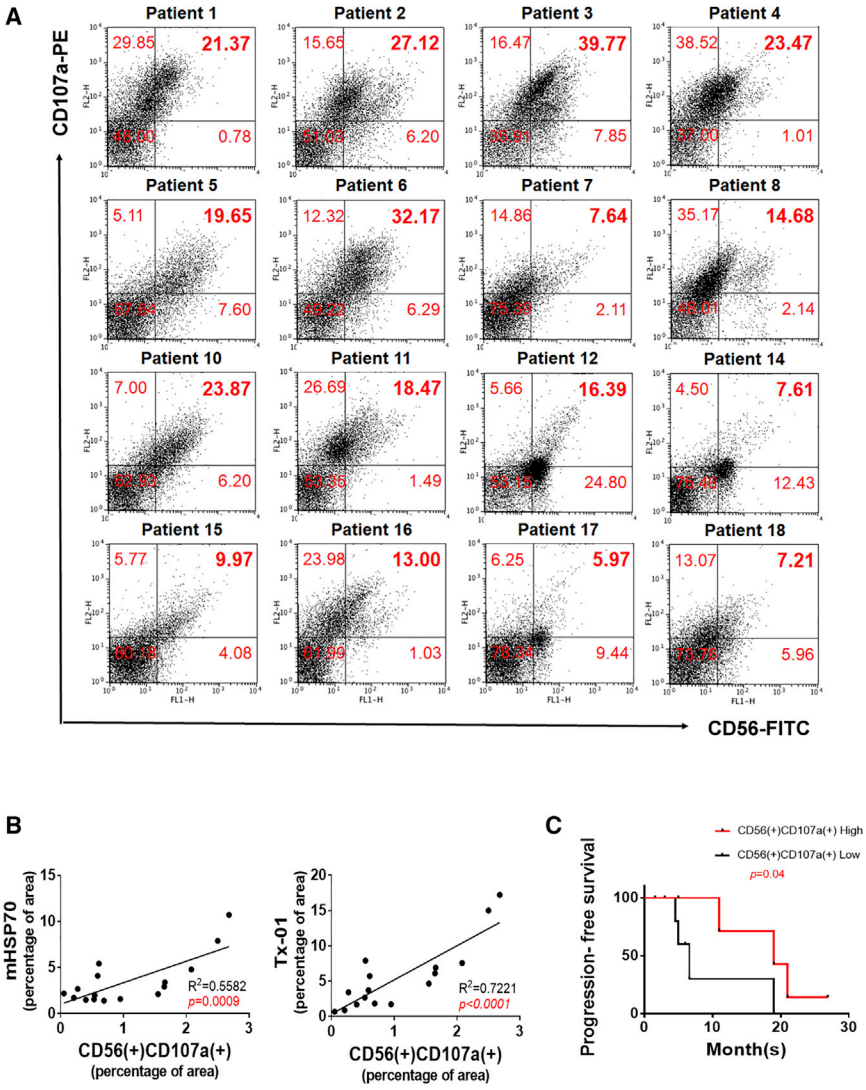

Figure 5. High CD56(+)CD107a(+) NK cells in the ascites led to favorable prognosis for serous OvCa patients

(A) After EpCAM-magnetic bead isolation, the EpCAM(–) cells were stained with anti-CD56 and anti-CD107a to detect activated NK cells [CD56(+)CD107a(+)] through flow cytometry. (B) The ascetic CD56(+)CD107a(+) activated NK cells were significantly and positively correlated with CTC mHSP70 expression (R^2 = 0.5582; p = 0.0009) and Tx-01 binding (R^2 = 0.7221; p < 0.0001). (C) Activated NK cells [CD56(+)CD107a(+)] were significantly associated with PFS (p = 0.04).

analyzed whether the CD56(+)CD107a(+) NK cell population in the ascites samples was associated with a good prognosis to evaluate the value of Tx-01 in OvCa predictions. Through flow cytometry analysis, we found that the proportions of CD56(+)CD107a(+) NK cells were different in the ascites from the 16 OvCa patients (Figure 5A). Furthermore, analyzing the immunofluorescence of the EpCAM(–) cells, we observed that patients may have had high CD56(+)CD107a(+) or low CD56(+)CD107a(+) NK cells in the ascites, as indicated by the median fluorescence area (= 0.65; Figure S5). Further, the mHSP70 and Tx-01 staining intensities were significantly and positively correlated with CD56(+)CD107a(+) NK cells (p = 0.0009, R^2 = 0.5582 and p < 0.0001, R^2 = 0.7221, respectively; Figure 5B). Using the median as the cutoff value (= 17.43) for high and low CD56(+)CD107a(+) activated NK cells in the ascites, we found that high CD56(+)CD107a(+) NK cells in the ascites were significantly associated with better PFS for patients (p = 0.04; Figure 5C). Overall, we demonstrated Tx-01 aptamer have both therapeutic and diagnostic roles in serous type OvCa. The possible molecular mechanism of Tx-01 in serous carcinoma is illustrated in Figure 6.

DISCUSSION

In this study, we demonstrated that the Tx-01 aptamer interacted with HSP70, showing dual roles as a therapeutic and prognostic factor for serous OvCa patients. Aptamers, selected via a SELEX process, can bind with target molecules selectively with high specificity and affinity and therefore can be used in diagnostic, therapeutic, imaging, and gene-regulatory applications.[5,6,25–27] Huh et al.[25] reported that colon cancer recurrence was successfully predicted for patients through array-based aptamer selection in a prognostic model. Macugen, an anti-vascular endothelial growth factor (VEGF) RNA aptamer, was demonstrated to be a prominent achievement in macular degeneration therapy.[26] Aptamers become essential targets for anticancer drug development because they are nontoxic and lack immunogenicity in contrast to antibodies.[28] OvCa, the most lethal cancer affecting women, has a poor 5-year survival rate, which has shown no improvement since 2008.[29] Developing new treatment modalities for this disease is important. Interestingly, we demonstrated that intracellular Tx-01 contributed to a decrease in HSP70/NICD translocation to the nucleus, which reduced cell migration and invasion (Figure 2). Because aptamers are small and specific oligonucleotides that can enter the intracellular space by endocytosis or pinocytosis,[30] they can interact with intracellular molecules, e.g., HSP70, with ease.

HSP70 is a chaperone protein that exhibits cytoprotective properties and is translocated to the nucleus under stress conditions.[31] Intracellular HSP70 can inhibit caspase activity directly or can be used indirectly against stress-induced apoptosis.[32] HSP70, which is found abundantly in cancers, suppresses apoptosis, allowing cancer to progress. Notably, a decrease in the level of HSP70-induced cancer cell death HSP70, which is found abundantly in cancers, suppresses

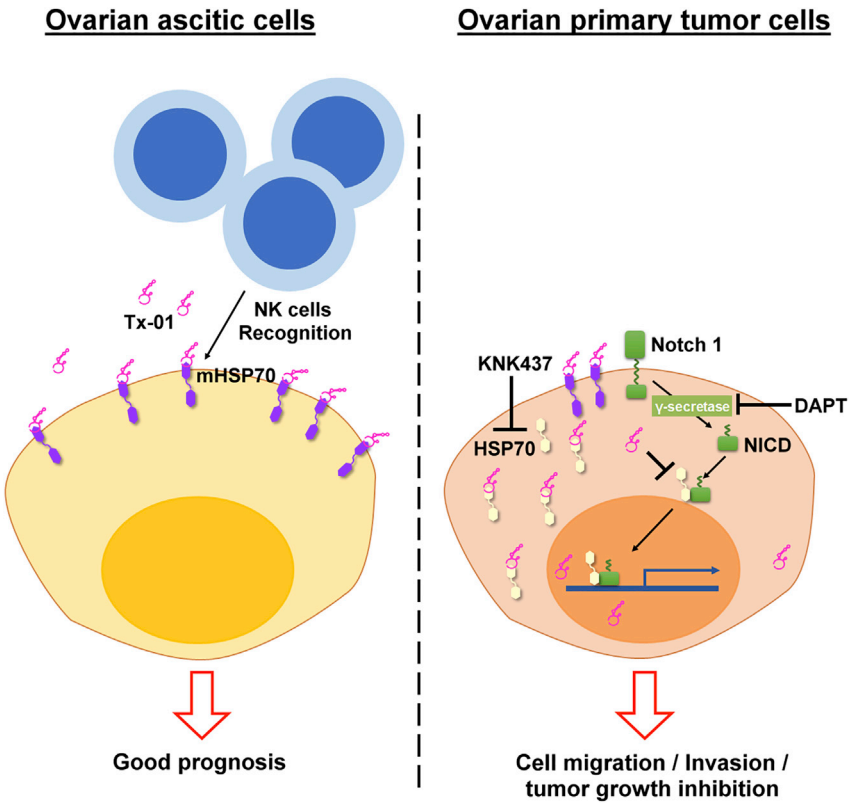

Figure 6. Diagram illustrating the dual role of Tx-01 in serous OvCa

In the ascitic CTCs, Tx-01 interacts with mHSP70, recognized by ascitic NK cell, and acts as a marker of good prognosis. Intracellular Tx-01 interrupts the interaction of HSP70 and NICD, blocking HSP70 nuclear translocation to reduce cell migration, invasion, and tumor growth.

apoptosis, allowing cancer to progress.[33] The overexpression of HSP70 has been linked to the aggressiveness of ovarian cancer.[34] Studies on effusions from OvCa patients revealed an association between HSP70 and poor overall survival.[35,36] In our serous OvCa cohort study, we found that high nuclear expression of HSP70 led to a poor prognosis (Figure 3E). Therefore, increasing cell apoptosis in cells by reducing intracellular HSP70 expression is a promising approach to cancer treatment. The high expression of HSP70 in serous OvCa may be a candidate target for Tx-01 treatment. In the xenograft mouse experiment (Figure 3), we demonstrated that Tx-01 is a novel therapeutic for use in serous OvCa with high HSP70 expression.

HSP70 has been reported to localize to the plasma membrane (mHSP70) under pathophysiological states, such as cancer, but not in corresponding normal cells.[13,14,37] Significant amounts of mHSP70 are often indicative of highly aggressive tumors, metastatic potential, and resistance to therapy, i.e., endometrial cancers, osteosarcomas, and renal cell tumors.[38,39] The role of mHSP70 as a target structure for NK cells has been demonstrated.[37] Tumor cells expressing mHSP70 are significantly more susceptible to NK-cell-mediated cell killing than those expressing low levels of mHsp70.[39] The importance of $CD8^+$ T cell infiltration in ovarian cancer tumors has been demonstrated, and the role of ascitic NK cells remains unclear.[40] Here, we observed Tx-01 on ascitic CTCs from 16 serous carcinoma patients, and it was significantly correlated with mHSP70 and CD56(+)CD107a(+) NK cells (Figure 4B). The results may be associated with the fact that mHSP70 is recognized by NK cells, leading to tumor cell death and a good outcome. However, the result of mHSP70 expression in PFS analysis showed borderline favorable prognosis ($p = 0.09$). The mHSP70 may not be sufficient to activate NK cells to cause tumor cells to be killed. The presence of cytokines, i.e., interleukin-2 (IL-2) or IL-15, is important for NK cell stimulation and activation.[41] One possible reason for borderline favorable prognosis between patients with mHSP70 high expression or low expression may be due to the different IL-2 or IL-15 level in patients' ascites. In addition, based on our previous study,[7] both GPM6a and BRCA2 may be possible binding targets of the Tx-01. In the Human Protein Atlas database, patients with high expressions of GPM6a or BRCA2 tend to have favorable prognosis than those with low expression. Overall, Tx-01 may be a good prognostic predictor of serous carcinoma through the recognition of mHSP70.

It is becoming increasingly clear that HSP70s are abundantly present in cancers, while the high HSP70 level causing it accumulates in lysosomes and then is transported to the membrane and released. For the mechanisms for Tx-01 aptamer into the intracellular space for its therapeutic effect, we conside that it binding with the mHSP70 on tumor cells surface and then rapid internalization after endocytosis or pinocytosis is another possibility action.[42]

In conclusion, in this study we demonstrated that the Tx-01 aptamer interacts with mHSP70 in ascitic CTCs as an NK cell recognition marker in serous carcinoma. On the other hand, Tx-01 reduced intracellular HSP70/NICD interactions to block HSP70 nuclear translocation and reduce cell migration and invasion. In terms of clinical treatment, the Tx-01 aptamer may be a potential candidate for a novel OvCa therapeutic modality, especially for serous OvCa with high levels of HSP70 expression. Tx-01 may have dual roles in serous OvCa prognosis prediction and therapy through its interaction with HSP70.

MATERIALS AND METHODS

Immunofluorescence staining and quantitation

IOSE-398, TOV-21G, and OVCAR3 cells were cultured in chamber slides and fixed in 4% paraformaldehyde for 15 min at room

temperature (RT). They were washed with ice-cold phosphate-buffered saline (PBS) and then incubated for 10 min in 0.25% Triton X-100 in (PBS). Bovine serum albumin (BSA; 1%) in PBS with Tween 20 (PBST) was then used for 30 min block the cells, and then Tx-01 aptamer (1:100; stock concentration = 100 nm, Genomics), anti-HSP70 (1:100; #4873; Cell Signaling), or anti-NICD (1:50; ab8925; Abcam) primary antibodies were added and stored overnight at 4°C. After washing with PBST, the samples were treated with fluorescence-conjugated secondary antibody in PBS for 1 h at RT in the dark. The results of the immunofluorescence staining were observed through a confocal microscope, and the percentage of the area with nuclear HSP70 was determined based on three different fields magnified 800× with ImageJ software.

Ascitic EpCAM(+) cells or CTCs were resuspended in 1% BSA containing Tx-01 aptamer (1:100; stock concentration = 100 nm, Genomics) and anti-HSP70 (1:100; sc-66048; Santa Cruz Biotechnology) antibodies incubated at RT for 1 h and then cytospinned on slides. The EpCAM(–) cells were collected and stained with anti-CD56 (1:50; #99746; Cell Signaling) and anti-CD107a (1:50; 328602; BioLegend) antibodies.

After washing with PBST, the samples were treated with fluorescence-conjugated secondary antibody in PBS for 1 h at RT in the dark. The immunofluorescence staining was observed using a ZEISS Axio Imager D2 microscope. The percentages of the areas stained with Tx-01, mHSP70, CD56, and CD107a were determined based on three different fields magnified at 200× with Nuance imaging software (version 3.0.2, PerkinElmer). To determine the colocalization of Tx-01/mHSP70 and CD56/CD107a (yellow), we further normalized the areas of Tx-01/mHSP70 and CD56/CD107a to the area stained by 4′,6-diamidino-2-phenylindole (DAPI).

IHC

For IHC analyses, paraffin-embedded samples from 113 serous-type ovarian cancer patients were immunostained with the anti-HSP70 antibody (1:500; CM407A; BioCare Medical). Then, horseradish peroxidase (HRP)-conjugated immunoglobulin G (IgG) antibody was added and incubated for 1 h, and the specimens were analyzed by using avidin and biotinylated enzyme complex (ABC) detection. The IHC images were observed under a ZEISS Axio Imager D2 microscope, and the nuclear HSP70 level was determined by using Nuance imaging software (version 3.0.2, PerkinElmer) based on three views of 200× field. This study was approved by the Human Experimental and Ethics Committee of NCKUH (IRB number A-ER-104-014) and Chi Mei Medical Center (IRB number 10807-005). Written informed consent for participation in the study was obtained from the participants.

LC-MS/MS

Total cell lysates or membrane proteins were prepared by using radioimmunoprecipitation assay (RIPA) buffer or a plasma membrane protein extraction kit following the manufacturer's instructions (ab65400, Abcam, UK).

Tx-01 aptamer-coated magnetic beads were incubated with 100 μg of cell lysate in a final volume of 350 μL for 1 h at RT. Protein/aptamer-bead complexes were then washed with PBS three times to remove nonspecifically bound proteins. Since the Tx-01 aptamer was modified with a biotin group at the 5′ end, the target molecules (i.e., binding sites) of aptamer Tx-01 were purified with streptavidin resin (G Bioscience, USA, Cat. #786-555). Finally, protein/aptamer-bead complexes were resuspended in double-distilled water (ddH_2O) containing 6× protein loading dye and heated at 95°C for 5 min followed by sodium dodecyl sulfate-polyacrylamide gel electrophoresis (SDS-PAGE) separation and staining with Coomassie brilliant blue. The protein candidates on the gels were subjected to trypsin digestion, and then the tryptic peptides were collected and desalted by C18 ZipTip column chromatography before the LC-MS analysis. Mass spectral data were acquired using a Thermo LTQ-Orbitrap Discovery Hybrid mass spectrometer (Thermo Fisher, USA) equipped with a nanoelectrospray ion source (New Objective, Woburn, MA, USA) and an Agilent 1200 Series binary high-performance LC (HPLC) pump (Agilent Technologies, USA). The experimental RAW files were converted to mgf format and subjected to Mascot analysis (version 2.3, Matrix Science, USA) to identify the target molecules of the Tx-01 aptamer. The methods were described previously by Vega et al.[12]

Western blot assay

30 μg of protein was subjected to 10% SDS-PAGE and transferred onto polyvinylidene fluoride (PVDF) membranes (IPVH00010; Millipore). The primary antibodies (Abs) were anti-HSP70 (1:1,000; #4873; Cell Signaling) and anti-activated Notch (NICD; 1:500; ab9825; Abcam). The secondary antibodies were anti-rabbit and anti-mouse HRP conjugates (1:10,000 dilution; A0545 and A9044; Sigma-Aldrich). The blocking/dilution reagent was 5% skim milk in a mixture of Tris-buffered saline plus 0.05% Tween 20 (TBST). The proteins were visualized using X-ray film and an enhanced chemiluminescence system (Millipore). The protein expression level was determined by using ImageJ software.

Tx-01 aptamers conjugated magnetic beads in pull-down assay

500 μL (800 mg) of stock Dynal streptavidin (SAv)-polystyrene-coated M280 (with a diameter of 2.8 μm) MBs (Thermo Fisher) were used for each sample and washed twice for 5 min each time with 1 mL of sterile PBS on a magnetic rack. The 5′-biotinylated Tx-01 aptamer was rehydrated in sterile PBS. Then, 100 μL of aptamer was added per 100 μL of stock SAv-MBs and mixed for 1 h at RT in sterile 1.5 mL microfuge tubes. The Tx-01 aptamer-5′-biotin-SAv-MBs were then collected on the magnetic rack for 2 min and then washed 3 times in 1 mL of sterile PBS. Tx-01-MBs were resuspended in 100 μL of sterile PBS, stored at 4°C, and then used in pull-down assays.

100 μL of stock Tx-01-MBs were added to each sample tube (with OVCAR3 or TOV-21G cell lysate). The tubes were mixed gently on a rotary mixer for 2 h at RT. The tubes were washed 3 times in 1 mL of sterile PBS per wash on a magnetic rack, and the mixtures

of Tx-01-MBs and cell lysate were collected. The interaction of Tx-01 and SHP70 was shown with immunoblotting.

Proximity ligation assay

The cells on coverslips were fixed in 4% paraformaldehyde for 10 min at RT, blocked with PBS, and 3% BSA for 1 h at 37°C and then costained overnight with 1 μM biotinylated Tx-01 and anti-HSP70 mouse monoclonal antibody (1:200 in PBS, Biocare Medical) at 4°C. Then, the coverslips were washed twice in PBS, and the cells were stained for 1 h with rabbit anti-biotin polyclonal antibody (1:200 in PBS with 3% BSA, Abcam) at 37°C. The coverslips were washed twice in PBS and subsequently stained with PLA probes (one anti-rabbit PLUS and one anti-mouse MINUS). According to the standard protocol using Duolink PLA technology, the interacting signal was amplified by using Duolink *in situ* red detection reagent. Finally, the coverslips were mounted in Prolong Gold mounting medium with DAPI and observed under a fluorescence microscope.

Flow cytometry

To analyze the Tx-01 interaction with membrane-bound HSP70, we used phycoerythrin (PE)-conjugated rat anti-HSP70 monoclonal antibody (1:100; 4873; Cell Signaling) and Tx-01 aptamer conjugated to Cy3 to stain TOV-21G or OVCAR3 cells, which were analyzed with FACS (BD Biosciences). Moreover, anti-CD56 (1:50; #99746; Cell Signaling), anti-CD107a (1:50; 328602; BioLegend), and suitable fluorescence-conjugated secondary Abs were used to determine the amount of activated NK cells through double staining. The geometric mean fluorescence intensity (MFI) was determined by FCSalyzer 0-5 software.

Isolation of the CTCs from OvCa patient ascites

Ascitic cells were collected by centrifugation at 1,500 revolutions per minute (rpm). These cells were suspended in PBS. Anti-EpCAM antibody (5 μL/test; 565398; BD Biosciences) was added and incubated for 1 h at RT. The negatively stained cells were removed after 1,500 rpm centrifugation, and positively stained cells were resuspended in 1× BD IMag buffer (10× dilution; 552362; BD Biosciences). 10 μL of anti-mouse IgG1 magnetic particles (10 μL/test; 557983; BD Biosciences) were added and incubated for 30 min at RT. The EpCAM(+) cells were collected by using a magnetic separator (552311; BD Biosciences) and resuspended in PBS for use in future experiments.

Migration/invasion assay

OVCAR3 cells (3×10^5) were seeded into a culture insert (IB-80209; ibid) or placed on 8-μm pore polycarbonate inserts containing Matrigel (354234; BD PharMingen) and incubated at 37°C. After 12 h, the migrating cells were observed and quantitated under a microscope by using ImageJ software; the membrane was slowly removed, washed in PBS, and stained with Giemsa. These invasive cells were counted under a microscope and photographed.

Xenograft mouse model

6-week-old nude (CAnN.Cg-*Foxn1*^{nu}/CrlNarl) mice were obtained from the National Laboratory Animal Center, Taiwan. The housing and experimental animal procedures were approved by the Institutional Animal Care and Use Committee of NCKU (approval number IACUC107197). OVCAR3 or TOV-21G cells (1×10^6/100 μL PBS) were subcutaneously injected into mice. Mice received no Tx-01 treatment (group A) or were injected with cells pretreated with Tx-01 only and then intratumorally treated with 100 μL of PBS twice a week (group B) or Tx-01 (200 nM/100 μL PBS) treatment twice a week (group C). The xenograft samples were immunostained with anti-HSP70 antibody (1:500; CM407A; BioCare Medical). The secondary antibodies, including HRP-conjugated IgG and fluorophore-conjugated IgG, were used for imaging. Nuance software version 3.0.2 (PerkinElmer) was used for quantification of the nuclear expression of HSP70 in the three groups.

Binding affinity assay

The binding affinity of HSP70 and NICD was measured by ELISA using a commercially available DIY kit (Rega Biotechnology). Recombinant human HSP70 (200 ng/well; AP-100; R&D Systems) was coated on a 96-well plate with 1× coating buffer (Rega Biotechnology). After incubation at 37°C for 1 h, the coating buffer was removed and the cells washed 3 times with 1× washing buffer (100 μL/well) and incubated at 37°C for 1 h. After removing the blocking buffer and washing buffer, equal volumes of Tx-01 (0 nM, 100 nM, 200 nM, 400 nM, 800 nM, and 1,600 nM) and NICD (1:5,000; ab8925; Abcam) were added and incubated overnight at 4°C. After removing the mixture of Tx-01 and NICD and washing buffer, rabbit IgG (1:10,000; 69610; Jackson ImmunoResearch, 100 μL/well) was added and incubated at 37°C for 1 h. After removing the rabbit IgG and washing buffer, the TMB substrate (100 μL/well) was added to the cells in the dark and incubated for 15 min, and then the absorbance at 570–595 nm was detected by an ELISA reader (Sunrise, TECAN).

Statistical analysis

The prognostic assessment was performed by time-dependent ROC, Kaplan-Meier survival, and Cox regression analyses (SPSS 26.0 and GraphPad 5 software) to determine significance differences. Statistical significance was set at $p < 0.05$. The data were expressed as the mean ± standard deviation (SD) based on three independent experiments. Statistical differences between means were analyzed using a paired or unpaired Student's t test.

SUPPLEMENTAL INFORMATION

Supplemental Information can be found online at https://doi.org/10.1016/j.omtn.2020.12.025.

ACKNOWLEDGMENTS

This work was supported by grants from the National Cheng Kung University Hospital (NCKUH-10801003), the Ministry of Science and Technology of Taiwan (MOST 106-2314-B-006-060-MY3 and MOST 107-2314-B-006-049), and partly by the National Health Research Institutes of Taiwan (NHRI-109A1-CACO-02202011). Author G.-B.L. thanks the National Health Research Institutes of Taiwan (NHRI-EX108-10728EI) for financial support. Partial

financial support from the "Higher Education Support Project" of Taiwan's Ministry of Education (grant number 108Q2713E1) and the Ministry of Science and Technology of Taiwan (MOST 107-2221-E-007-013-MY3) is also greatly appreciated.

AUTHOR CONTRIBUTIONS

Conception and design: C.-N.L., Y.-C.T., C.-C.H., and K.-F.H. Development of methodology: C.-N.L., Y.-C.T., C.-C.H., Y.-Y.W., and P.-H.H. Acquisition of data (provided animals, acquired and managed patient data, provided facilities, etc.): Y.-L.L., C.-Y.K., C.-H.L., G.-B.L., and K.-F.H. Analysis and interpretation of data (e.g., statistical analysis, biostatistics, computational analysis): Y.-L.L. and C.-N.L. Writing, review, and/or revision of the manuscript: C.-N.L., Y.-C.T., C.-C.H., Y.-Y.W., and K.-F.H. Administrative, technical, or material support (i.e., reporting or organizing data, constructing databases): C.-N.L., Y.-C.T., G.-B.L., and K.-F.H. Study supervision: G.-B.L. and K.-F.H.

DECLARATION OF INTERESTS

The authors declare no competing interests.

REFERENCES

1. Malvezzi, M., Carioli, G., Rodriguez, T., Negri, E., and La Vecchia, C. (2016). Global trends and predictions in ovarian cancer mortality. Ann. Oncol. *27*, 2017–2025.
2. Siegel, R.L., Miller, K.D., and Jemal, A. (2019). Cancer statistics, 2019. CA Cancer J. Clin. *69*, 7–34.
3. Bowtell, D.D. (2010). The genesis and evolution of high-grade serous ovarian cancer. Nat. Rev. Cancer *10*, 803–808.
4. Berchuck, A., Secord, A.A., Moss, H.A., and Havrilesky, L.J. (2017). Maintenance Poly (ADP-ribose) Polymerase Inhibitor Therapy for Ovarian Cancer: Precision Oncology or One Size Fits All? J. Clin. Oncol. *35*, 3999–4002.
5. Sun, H., Zhu, X., Lu, P.Y., Rosato, R.R., Tan, W., and Zu, Y. (2014). Oligonucleotide aptamers: new tools for targeted cancer therapy. Mol. Ther. Nucleic Acids *3*, e182.
6. Meirinho, S.G., Dias, L.G., Peres, A.M., and Rodrigues, L.R. (2017). Electrochemical aptasensor for human osteopontin detection using a DNA aptamer selected by SELEX. Anal. Chim. Acta *987*, 25–37.
7. Hung, L.Y., Fu, C.Y., Wang, C.H., Chuang, Y.J., Tsai, Y.C., Lo, Y.L., Hsu, P.H., Chang, H.Y., Shiesh, S.C., Hsu, K.F., and Lee, G.B. (2018). Microfluidic platforms for rapid screening of cancer affinity reagents by using tissue samples. Biomicrofluidics *12*, 054108.
8. Huang, S.P., Chuang, Y.J., Lee, W.B., Tsai, Y.C., Lin, C.N., Hsu, K.F., and Lee, G.B. (2020). An integrated microfluidic system for rapid, automatic and high-throughput staining of clinical tissue samples for diagnosis of ovarian cancer. Lab Chip *20*, 1103–1109.
9. Sherman, M.Y., and Gabai, V.L. (2015). Hsp70 in cancer: back to the future. Oncogene *34*, 4153–4161.
10. Gupta, N., Jagadish, N., Surolia, A., and Suri, A. (2017). Heat shock protein 70-2 (HSP70-2) a novel cancer testis antigen that promotes growth of ovarian cancer. Am. J. Cancer Res. *7*, 1252–1269.
11. Seigneuric, R., Mjahed, H., Gobbo, J., Joly, A.L., Berthenet, K., Shirley, S., and Garrido, C. (2011). Heat shock proteins as danger signals for cancer detection. Front. Oncol. *1*, 37.
12. Vega, V.L., Rodríguez-Silva, M., Frey, T., Gehrmann, M., Diaz, J.C., Steinem, C., Multhoff, G., Arispe, N., and De Maio, A. (2008). Hsp70 translocates into the plasma membrane after stress and is released into the extracellular environment in a membrane-associated form that activates macrophages. J. Immunol. *180*, 4299–4307.
13. Gehrmann, M., Liebisch, G., Schmitz, G., Anderson, R., Steinem, C., De Maio, A., Pockley, G., and Multhoff, G. (2008). Tumor-specific Hsp70 plasma membrane localization is enabled by the glycosphingolipid Gb3. PLoS ONE *3*, e1925.
14. Multhoff, G., Botzler, C., Wiesnet, M., Müller, E., Meier, T., Wilmanns, W., and Issels, R.D. (1995). A stress-inducible 72-kDa heat-shock protein (HSP72) is expressed on the surface of human tumor cells, but not on normal cells. Int. J. Cancer *61*, 272–279.
15. Stangl, S., Gehrmann, M., Riegger, J., Kuhs, K., Riederer, I., Sievert, W., Hube, K., Mocikat, R., Dressel, R., Kremmer, E., et al. (2011). Targeting membrane heat-shock protein 70 (Hsp70) on tumors by cmHsp70.1 antibody. Proc. Natl. Acad. Sci. USA *108*, 733–738.
16. Breuninger, S., Stangl, S., Werner, C., Sievert, W., Lobinger, D., Foulds, G.A., Wagner, S., Pickhard, A., Piontek, G., Kokowski, K., et al. (2018). Membrane Hsp70-A Novel Target for the Isolation of Circulating Tumor Cells After Epithelial-to-Mesenchymal Transition. Front. Oncol. *8*, 497.
17. Multhoff, G., Pfister, K., Gehrmann, M., Hantschel, M., Gross, C., Hafner, M., and Hiddemann, W. (2001). A 14-mer Hsp70 peptide stimulates natural killer (NK) cell activity. Cell Stress Chaperones *6*, 337–344.
18. Gastpar, R., Gross, C., Rossbacher, L., Ellwart, J., Riegger, J., and Multhoff, G. (2004). The cell surface-localized heat shock protein 70 epitope TKD induces migration and cytolytic activity selectively in human NK cells. J. Immunol. *172*, 972–980.
19. Hoogstad-van Evert, J.S., Maas, R.J., van der Meer, J., Cany, J., van der Steen, S., Jansen, J.H., Miller, J.S., Bekkers, R., Hobo, W., Massuger, L., and Dolstra, H. (2018). Peritoneal NK cells are responsive to IL-15 and percentages are correlated with outcome in advanced ovarian cancer patients. Oncotarget *9*, 34810–34820.
20. Yuan, X., Wu, H., Xu, H., Xiong, H., Chu, Q., Yu, S., Wu, G.S., and Wu, K. (2015). Notch signaling: an emerging therapeutic target for cancer treatment. Cancer Lett. *369*, 20–27.
21. Groeneweg, J.W., Foster, R., Growdon, W.B., Verheijen, R.H., and Rueda, B.R. (2014). Notch signaling in serous ovarian cancer. J. Ovarian Res. *7*, 95.
22. Alniaimi, A.N., Demorest-Hayes, K., Alexander, V.M., Seo, S., Yang, D., and Rose, S. (2015). Increased Notch1 expression is associated with poor overall survival in patients with ovarian cancer. Int. J. Gynecol. Cancer *25*, 208–213.
23. Juryńczyk, M., Lewkowicz, P., Domowicz, M., Mycko, M.P., and Selmaj, K.W. (2015). Heat shock protein 70 (Hsp70) interacts with the Notch1 intracellular domain and contributes to the activity of Notch signaling in myelin-reactive CD4 T cells. J. Neuroimmunol. *287*, 19–26.
24. Hooda, J., Novak, M., Salomon, M.P., Matsuba, C., Ramos, R.I., MacDuffie, E., Song, M., Hirsch, M.S., Lester, J., Parkash, V., et al. (2019). Early Loss of Histone H2B Monoubiquitylation Alters Chromatin Accessibility and Activates Key Immune Pathways That Facilitate Progression of Ovarian Cancer. Cancer Res. *79*, 760–772.
25. Huh, J.W., Kim, S.C., Sohn, I., Jung, S.H., and Kim, H.C. (2016). Serum protein profiling using an aptamer array predicts clinical outcomes of stage IIA colon cancer: A leave-one-out crossvalidation. Oncotarget *7*, 16338–16348.
26. Ng, E.W., Shima, D.T., Calias, P., Cunningham, E.T., Jr., Guyer, D.R., and Adamis, A.P. (2006). Pegaptanib, a targeted anti-VEGF aptamer for ocular vascular disease. Nat. Rev. Drug Discov. *5*, 123–132.
27. Wurster, S.E., and Maher, L.J., 3rd (2008). Selection and characterization of anti-NF-kappaB p65 RNA aptamers. RNA *14*, 1037–1047.
28. Chen, C., Zhou, S., Cai, Y., and Tang, F. (2017). Nucleic acid aptamer application in diagnosis and therapy of colorectal cancer based on cell-SELEX technology. NPJ Precis. Oncol. *1*, 37.
29. Coleman, R.L., Monk, B.J., Sood, A.K., and Herzog, T.J. (2013). Latest research and treatment of advanced-stage epithelial ovarian cancer. Nat. Rev. Clin. Oncol. *10*, 211–224.
30. Thierry, A.R., Vives, E., Richard, J.P., Prevot, P., Martinand-Mari, C., Robbins, I., and Lebleu, B. (2003). Cellular uptake and intracellular fate of antisense oligonucleotides. Curr. Opin. Mol. Ther. *5*, 133–138.
31. Nollen, E.A., Salomons, F.A., Brunsting, J.F., van der Want, J.J., Sibon, O.C., and Kampinga, H.H. (2001). Dynamic changes in the localization of thermally unfolded nuclear proteins associated with chaperone-dependent protection. Proc. Natl. Acad. Sci. USA *98*, 12038–12043.

32. Mosser, D.D., Caron, A.W., Bourget, L., Meriin, A.B., Sherman, M.Y., Morimoto, R.I., and Massie, B. (2000). The chaperone function of hsp70 is required for protection against stress-induced apoptosis. Mol. Cell. Biol. *20*, 7146–7159.

33. Nylandsted, J., Rohde, M., Brand, K., Bastholm, L., Elling, F., and Jäättelä, M. (2000). Selective depletion of heat shock protein 70 (Hsp70) activates a tumor-specific death program that is independent of caspases and bypasses Bcl-2. Proc. Natl. Acad. Sci. USA *97*, 7871–7876.

34. Annunziata, C.M., Kleinberg, L., Davidson, B., Berner, A., Gius, D., Tchabo, N., Steinberg, S.M., and Kohn, E.C. (2007). BAG-4/SODD and associated antiapoptotic proteins are linked to aggressiveness of epithelial ovarian cancer. Clin. Cancer Res. *13*, 6585–6592.

35. Cohen, M., Dromard, M., and Petignat, P. (2010). Heat shock proteins in ovarian cancer: a potential target for therapy. Gynecol. Oncol. *119*, 164–166.

36. Elstrand, M.B., Kleinberg, L., Kohn, E.C., Tropé, C.G., and Davidson, B. (2009). Expression and clinical role of antiapoptotic proteins of the bag, heat shock, and Bcl-2 families in effusions, primary tumors, and solid metastases in ovarian carcinoma. Int. J. Gynecol. Pathol. *28*, 211–221.

37. Multhoff, G., Botzler, C., Jennen, L., Schmidt, J., Ellwart, J., and Issels, R. (1997). Heat shock protein 72 on tumor cells: a recognition structure for natural killer cells. J. Immunol. *158*, 4341–4350.

38. Murakami, N., Kühnel, A., Schmid, T.E., Ilicic, K., Stangl, S., Braun, I.S., Gehrmann, M., Molls, M., Itami, J., and Multhoff, G. (2015). Role of membrane Hsp70 in radiation sensitivity of tumor cells. Radiat. Oncol. *10*, 149.

39. Ciocca, D.R., and Calderwood, S.K. (2005). Heat shock proteins in cancer: diagnostic, prognostic, predictive, and treatment implications. Cell Stress Chaperones *10*, 86–103.

40. Hoogstad-van Evert, J.S., Bekkers, R., Ottevanger, N., Jansen, J.H., Massuger, L., and Dolstra, H. (2020). Harnessing natural killer cells for the treatment of ovarian cancer. Gynecol. Oncol. *157*, 810–816.

41. Albakova, Z., Armeev, G.A., Kanevskiy, L.M., Kovalenko, E.I., and Sapozhnikov, A.M. (2020). HSP70 Multi-Functionality in Cancer. Cells *9*, 587.

42. Gehrmann, M., Stangl, S., Foulds, G.A., Oellinger, R., Breuninger, S., Rad, R., Pockley, A.G., and Multhoff, G. (2014). Tumor imaging and targeting potential of an Hsp70-derived 14-mer peptide. PLoS ONE *9*, e105344.